Three-Dimensional Solution Structure of *Acanthamoeba* Profilin-I

Valda K. Vinson,* Sharon J. Archer,‡ Eaton E. Lattman,§ Thomas D. Pollard,* and Dennis A. Torchia‡

*Department of Cell Biology and Anatomy, The Johns Hopkins University School of Medicine, Baltimore, Maryland 21205; ‡Bone Research Branch, National Institute of Dental Research, National Institutes of Health, Bethesda, Maryland 20892; and §Department of Biophysics and Biophysical Chemistry, The Johns Hopkins University School of Medicine, Baltimore, Maryland 21205

Abstract. We have determined a medium resolution three-dimensional solution structure of *Acanthamoeba* profilin-I by multidimensional nuclear magnetic resonance spectroscopy. This 13-kD actin binding protein consists of a five stranded antiparallel beta sheet flanked by NH_2- and COOH-terminal helices on one face and by a third helix and a two stranded beta sheet on the other face. Data from actin-profilin cross-linking experiments and the localization of conserved residues between profilins in different phyla indicate that actin binding occurs on the molecular face occupied by the terminal helices. The other face of the molecule contains the residues that differ between *Acanthamoeba* profilins-I and II and may be important in determining the difference in polyphosphoinositide binding between these isoforms. This suggests that lipids and actin bind to different faces of the molecule.

PROFILINS (Carlsson et al., 1977; Reichstein and Korn, 1979) are highly abundant, low molecular weight cytoplasmic proteins that form a polyphosphoinositide sensitive complex with actin monomers (Lassing and Lindberg, 1985, 1988). Profilins regulate actin polymerization directly by binding to actin monomers with micromolar affinities (Pollard and Cooper, 1986) and possibly binding to the barbed end of actin filaments to form a weak cap (Pollard and Cooper, 1984). In addition, profilins inhibit actin nucleation and catalytically increase the rate of exchange of the actin ligands ATP and Ca^{2+} (Goldschmidt-Clermont et al., 1991*b*; Mockrin and Korn, 1980; Nishida, 1985). By binding to phosphoatidylinositol-4,5-biphosphate (PIP_2)[1], profilins inhibit the production of the second messengers inositol trisphosphate and diacylglycerol by unphosphorylated phospholipase C-γ1 (Goldschmidt-Clermont et al., 1990; Machesky et al., 1990). Phosphorylation of phospholipase C-γ1 by the epidermal growth factor receptor tyrosine kinase overcomes this inhibition by profilin (Goldschmidt-Clermont et al., 1991*a*). This provides a biochemical mechanism to couple growth factor binding to its receptor with the production of these second messengers. Because PIP_2 inhibits the binding of profilin to actin (Lassing and Lindberg, 1985, 1988), profilin may link transmembrane signaling and regulation of the cytoskeleton. Genetic evidence that profilin function is required for cytoskeletal integrity was first provided by disruption of the profilin encoding *Saccharomyces cerevisiae* PFY gene. PFY^- cells bud randomly and have defective actin distribution (Haarer et al., 1990). Further evidence that profilin is involved in a signaling pathway is that overexpression of PFY in *S. cerevisiae* suppresses morphological and nutritional defects associated with loss of the COOH-terminal domain of CAP (Vojtek et al., 1991), a bifunctional signal transduction protein. Profilin also binds polymers of L-proline in vitro (Tanaka and Shibata, 1985) suggesting that it has an additional, as yet unidentified, function.

Acanthamoeba has three isoforms of profilin, IA, IB and II (Ampe et al., 1985; Kaiser et al., 1986). Profilin-IA[2], the most abundant isoform, is acidic with an isoelectric point of 5.5, whereas profilin-II is basic with an isoelectric point >9 (Kaiser et al., 1986). Profilin-IB differs only slightly from IA (Ampe et al., 1985; Pollard and Rimm, 1991). Profilins from *Acanthamoeba castellanii* can be overexpressed in bacteria (Kaiser, D. A., M. Way, S. Almo, and T. D. Pollard, manuscript in preparation) and isotopically labeled in quantities required for structural determination by heteronuclear NMR techniques.

Atomic structures are essential for understanding the complex molecular interactions of profilins, but no three-dimensional structure of profilin has been reported. Single crystals of *Acanthamoeba* profilin (Magnus et al., 1986) and

Address correspondence to Dennis A. Torchia, National Institutes of Health, Building 30, Room 106, Bethesda, MD 20892.

1. *Abbreviations used in this paper*: HMQC, heteronuclear multiple quantum correlation; HOHAHA, homonuclear Hartmann-Hahn; HSQC, heteronuclear single quantum correlation; NMR, nuclear magnetic resonance; NOE, nuclear Overhauser effect; PIP_2, phosphatidylinositol-4,5-biphosphate; ROESY, rotating frame Overhauser effect spectroscopy.

2. Profilin IA: SWQTYVDTNLVGTGAVTQAAILGLDGNTWATSAGFAVTPAQGQTLASAFNNADPIRASGFDLAGVHYVTLRADDRSIYGKKGSAGVITVKTSKSILVGVYNEKIQPGTAANVVEKLADYLIGQGF (Pollard and Rimm, 1991).

the actin profilin complex of human profilin (Schutt et al., 1989) have been available for several years, but technical problems have hindered structure determination.

Over the last decade, NMR spectroscopy has proven to be a reliable technique for determining the structure of proteins in solution (Clore and Gronenborn, 1991; Wüthrich, 1989). The first step in determining the structure of proteins in solution is to assign the NMR signals to particular atoms in the protein. Once NMR signal assignments are known, NOE and coupling constant information is used to determine the secondary and the three-dimensional structure of the protein in solution. We have previously reported the NMR signal assignments and secondary structure of *Acanthamoeba* profilin IA (Archer et al., 1993). Herein we report the three-dimensional structure of this 125 residue protein as determined using additional nuclear Overhauser effect (NOE) and coupling constant information.

Materials and Methods

Samples of recombinant *Acanthamoeba* profilin-I uniformly enriched with ^{15}N or with ^{15}N and ^{13}C were obtained by bacterial expression of profilin in minimal media containing $^{15}NH_4Cl$ or $^{15}NH_4Cl/^{13}C$ glucose, respectively, as described previously (Archer et al., 1993). All samples used for NMR experiments contained ~1.3 mM protein in D_2O or 93% H_2O/7% D_2O, pH 6.4. NMR spectra were acquired on Bruker AMX500 and AMX600 spectrometers at 30°C unless noted otherwise.

NOEs were determined from the following three- and four-dimensional heteronuclear NOESY experiments: three-dimensional ^{15}N separated NOESY-HMQC, $^{13}C/^{15}N$ separated NOESY-HMQC and four-dimensional $^{13}C/^{13}C$ separated HMQC-NOESY-HMQC. The NOE mixing times were either 70 or 110 ms. Acquisition parameters and examples of the quality of the spectra on profilin have been published previously (Archer et al., 1993). In addition, a three-dimensional ^{15}N separated ROESY-HMQC (Clore et al., 1990) spectrum was acquired with a 35 ms ROE mixing time. The ROESY-HMQC spectrum was acquired with spectral widths of 10.00, 22.9, and 11.76 in $F_1(^1H)$, $F_2(^{15}N)$, and $F_3(^1H)$, respectively, and with 120 complex points in t_1, 32 complex points in t_2, 512 complex points in t_3, and 32 scans per t_3 point.

$^3J_{HNH\alpha}$ coupling constants were calculated from splittings in a two-dimensional HMQC-J (Kay and Bax, 1990) experiment and H_α/H_N intensity ratios in a short mixing time (30 ms) three-dimensional HOHAHA-HSQC (Marion et al., 1989) experiment as reported previously (Archer et al., 1993). For H_α peaks near the water resonance, $^3J_{HNH\alpha}$ coupling constants were calculated from H_α/H_N intensity ratios in an HNHA (Vuister and Bax, 1993) experiment. $^3J_{NH\beta}$ couplings were determined qualitatively from a three-dimensional HNHB (Archer et al., 1991) and $^3J_{NC\gamma}$ couplings were calculated from a two-dimensional [^{15}N] spin echo difference CT-HSQC (Vuister, G., A. C. Wang, and A. Bax, submitted for publication) experiment.

The NOEs were classified as strong, medium, weak or very weak. These relative intensities were interpreted as distance constraints as follows: strong <2.7 Å; medium <3.3 Å; weak <4.3 Å; very weak <5.0 Å following the protocol of Clore et al. (1986). A correction was added to the upper limit for constraints involving methyl protons and nonstereospecifically assigned protons (Clore et al., 1987; Wüthrich et al., 1983). Stereospecific assignments of $H\beta$ resonances were based on quantitative measurements of $^3J_{NH\beta}$ and $^3J_{NC\gamma}$ coupling constants, as well as qualitative determination of $^3J_{H\alpha H\beta}$ couplings from three-dimensional HOHAHA-HSQC spectra and intraresidue NOEs. Determination of ϕ and χ_1 torsion angle restraints were based on NOEs and $^3J_{HNH\alpha}$, $^3J_{NH\beta}$, and $^3J_{NC\gamma}$ coupling constants. ϕ torsion angles were constrained between −30 and −90° for $^3J_{HNH\alpha}$ values <6 Hz and between −80 and −160° for $^3J_{HNH\alpha}$ values >8 Hz and χ_1 angles were restricted to a ±60°C range.

Structures were calculated using the hybrid distance geometry-dynamical simulated annealing method of Nilges et al. (1988) as contained in the program X-PLOR 3.0 (Brünger, 1992). A template structure was generated with an arbitrary extended conformation using the X-PLOR routine *generate-template*. A subset of atoms from this template were embedded into the distance and torsion angle constraint matrix using the X-PLOR routine *dg-sub-embed*, which was followed by a combination of distance geometry and simulated annealing on the full structure using the routine *dgsa*.

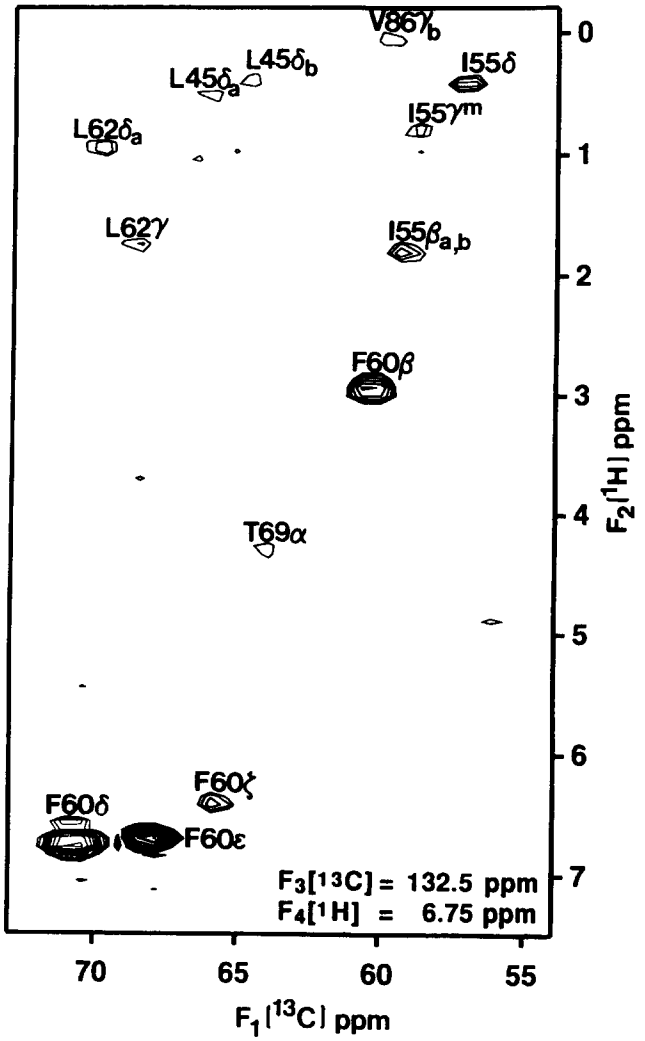

Figure 1. An $F_4(^1H)$-$F_3(^{13}C)$ plane from the 4D NOESY experiment at the $^1H^\delta$-$^{13}C^\delta$ chemical shifts of Phe^{60}. The spectrum was recorded at 600 MHz as a four-dimensional matrix of 16 × 64 × 17 × 384 complex points with spectral widths of 20.7, 8.96, 20.7, and 11.90 ppm in $F_1(^{13}C)$, $F_2(^1H)$, $F_3(^{13}C)$ and $F_4(^1H)$, respectively. Cross-peaks on this plane arise from protons that are close in space to the H^δ of Phe^{60}. Intraresidue connectivities, short range connectivities to Leu^{62}, and long range connectivities to Leu^{45}, Ile^{55}, Thr^{69} and Val^{86} are observed. Tertiary interactions between secondary structure elements are defined by the cross-peaks between Phe^{60} (in the two-stranded β-sheet) and both Val^{86} (in the five-stranded β-sheet) and Leu^{45} (in helix 2). Note that the spectrum is extensively folded in the ^{13}C dimensions so that ^{13}C chemical shifts are given by x±nSW, where x is the ppm value in the figure, *n* is an integer, and SW is the spectral width (20.7 ppm).

The structures were then refined using the routine *refine* and only those structures with minimal NOE distance and torsion angle violations were kept. In an iterative fashion, an initial set of structures was used to assign previously ambiguous NOE distance constraints which were added to the constraints and used to generate a new set of structures (Clore and Gronenborn, 1989). 13 final structures met the criteria of no significant (>0.5 Å) NOE constraint violations and at most one dihedral constraint violation >5°. Of these 13 structures, the 12 structures that overlay the closest were chosen.

Results

The final set of structures was based on a total of 915 struc-

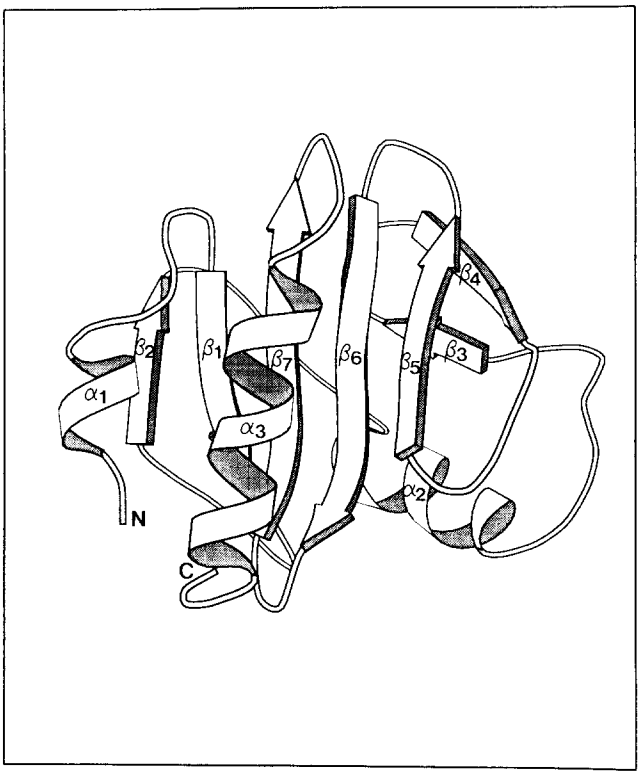

Figure 2. (*A*) Overlay of 12 refined profilin-I structures. The trace of the α-carbon atoms is shown, with α-helices colored purple and β-sheets colored yellow. All 125 amino acid residues were included in structure determinations, but the two NH_2-terminal and four COOH-terminal residues, which are disordered, were excluded for calculation of RMSDs. The average RMSDs to a mean structure are 1.2 Å for the backbone atoms and 1.7 Å for all heavy atoms. Most variation between structures occurs in the loop regions (*blue*). (*B*) Schematic representation showing the topography of profilin-I drawn using MOLSCRIPT software (Kraulis, 1991). Secondary structure elements are labeled. Note that the two NH_2-terminal and four COOH-terminal residues are ill-defined.

A

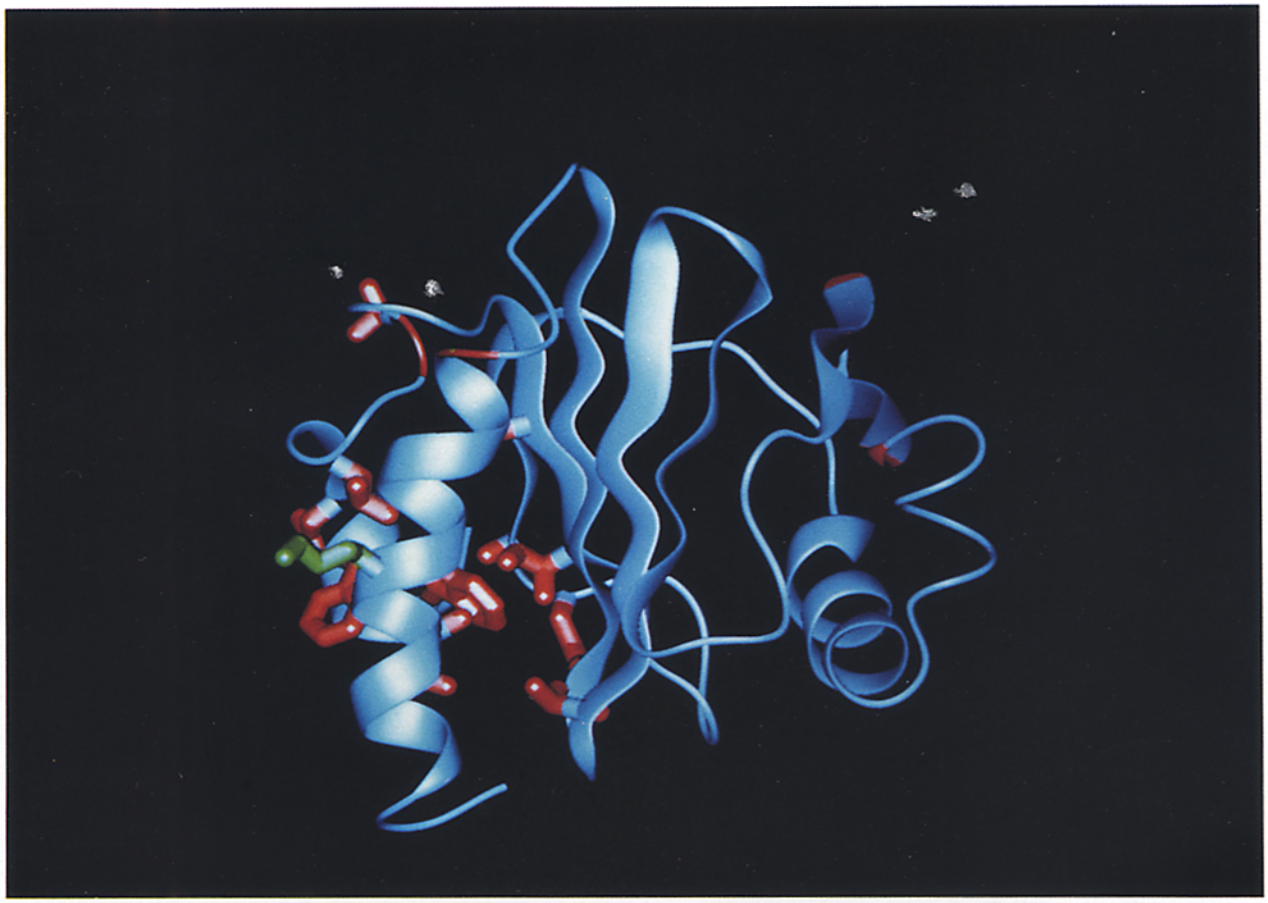

B

turally significant distance constraints; 556 of these were interresidue restraints of which 184 were long range, involving residues separated by at least five amino acids in the primary sequence. The NMR signal assignments and secondary structure of *Acanthamoeba* profilin I based on NOEs, coupling constants and hydrogen exchange rates were reported previously (Archer et al., 1993). These constraints plus additional NOEs obtained from a 110 ms four-dimensional $^{13}C/^{13}C$ separated HMQC-NOESY-HMQC experiment were used to determine the NOE distance constraints. A plane from the four-dimensional NOESY data set illustrates the high quality NOE data used to determine these additional NOE constraints (Fig. 1). In addition, 55 backbone ϕ angle restraints and 23 side chain χ_1 angle restraints were used. 40 hydrogen bonds were included as constraints in cases where both NOE correlations and hydrogen exchange data were consistent with hydrogen bonding.

In 12 refined structures (Fig. 2 *A*), the elements of secondary structure, especially the central five-stranded β-sheet, overlay closely. The backbone coordinates for this family of 12 structures have been deposited with the Protein Data Bank, Chemistry Department, Brookhaven National Laboratory (Upton, NY), from which copies are available. Interproton distances that are outside the lower or upper bounds of distance constraints are reported as violations. Each of the refined structures has no violations of NOE constraints >0.5 Å and no more than four violations >0.3 Å. On average, each structure had one or two violations above 0.3 Å. A mean structure was determined by averaging the coordinates of the 12 structures. The average root mean square deviations of these 12 structures to the mean structure are 1.2 Å for the backbone atoms and 1.7 Å for all heavy atoms. Superposition of only the regions with regular secondary structure gives average RMSDs of 0.9 Å for backbone atoms and 1.4 Å for all heavy atoms. The highest resolution protein structures yet attained by NMR methods have backbone atom RMSDs of 0.4–0.5 Å (Clore and Gronenborn, 1991). While we are working to obtain this level of resolution, the current medium resolution structure provides new and significant information about the overall tertiary fold of profilin that provides the first insights into the relationship between the three-dimensional structure and the function in profilin-I.

The central topological feature of *Acanthamoeba* profilin-I is a five-stranded antiparallel β-sheet. Two helices located near the NH_2 and COOH termini, respectively, lie parallel to one another on one side of the five-stranded β-sheet; a third helix and a two stranded antiparallel β-sheet lie on the other side of the five-stranded β sheet (Fig. 2 *B*). The seven β-strands extend between residues Gln[18]-Leu[22], Ala[30]-Ala[33], Phe[60]-Leu[62], Val[65]-Tyr[67], Ser[76]-Lys[81], Ala[84]-Thr[91] and Ser[94]-Asn[101]. The five-stranded antiparallel β-sheet is made up of strands 2, 1, 7, 6, 5, and the two-stranded antiparallel β-sheet comprises strands 3 and 4—where the strands are numbered sequentially according to the primary sequence. The three well-defined helices include an NH_2-terminal α helix involving residues Gln[3]-Asp[7](α_1), a long COOH-terminal α helix spanning residues Ala[109]-Ile[121] (α_3), and an α helix comprising residues Ala[40]-Phe[49](α_2) (Fig. 2 *B*).

The position of the NH_2 terminus is not well defined because, as is typical of proteins in solution, the amide protons of the first two resonances, Ser[1] and Trp[2], were in fast exchange with the solvent and were not observed by NMR. However, the position of Trp[2] is well defined because of several long range NOE constraints to the aromatic side chain. Residues Gln[3] to Asp[7] form a well defined α-helix (α_1) which is followed by helixlike turns for residues Thr[8] to Val[16]. However, not all residues in this segment of the sequence show $H_{\alpha i}$-$H_{\beta i+3}$ and $H_{\alpha i}$-H_{Ni+3} NOEs or small $^3J_{HN\alpha}$ coupling constants typical of canonical α-helical structures. Furthermore, residues 11–14 are not well constrained by the NMR data and show RMSD's of 2 Å when the backbones of the structures are compared. After residue Val[16], the chain turns back on itself and forms the first β-strand (β_1) from Gln[18] to Leu[22]. Residues Gly[23] to Thr[28] form a loop followed by the second β-strand (β_2) which extends between residues Ala[30] and Ala[33]. At the end of this strand the chain turns through ~60° and forms a relatively extended structure between Gly[34] and Ala[40]. Residues Ala[40] to Phe[49] form a well-defined α-helix (α_2). The helix ends before Asn[50] which has a large $^3J_{HN\alpha}$ coupling constant and Asn[51] is in an extended conformation. Residues Asp[53] to Arg[56] form a helical turn which is characterized by two weak $H_{\alpha i}$ to $H_{\beta i+3}$ NOEs and upfield shifted C_2 chemical shifts characteristic of helices. Residues Phe[60] to Leu[62] form an extended β-strand (β_3) followed by a tight turn at residues Ala[63] and Gly[64] and a β-strand antiparallel to β3 between residues Val[65] and Val[68] (β_4). The loop region between residues Asn[50] and Gly[59] reverses the direction of the polypeptide chain so that the two-stranded β-sheet between residues Phe[60] and Val[68] is parallel to the second α-helix (α_2). After the β_4 strand, the backbone is extended at Thr[69] and then bulges at Leu[70] and Arg[71]. Residues Ala[72] and Asp[73] are in an extended conformation and display hydrogen bonds to Ile[77] and Ser[76], respectively, which are in the β_5 strand. A reverse turn at residues Asp[74] and Arg[75] accommodates the chain folding back on itself. Residues Ser[76] to Lys[81] form an extended β-strand (β_5). A reverse turn at residues Gly[82] and Ser[83] allows the chain to fold back on itself to accommodate the next strand (β_6) (residues Ala[84] to Thr[91]) in the antiparallel β-sheet. Residues Ser[92] and Lys[93] comprise the tight turn that leads into a third consecutive strand in the β-sheet: Ser[94] to Asn[101] (β_7). Residues Glu[102] to Thr[108] form a loop which leads into a well-defined COOH-terminal helix comprising residues Ala[109] to Ile[121] (α_3). The four COOH-terminal residues form a helixlike turn, but do not display connectivities characteristic of canonical α-helical structure.

Packing of the NH_2- and COOH-terminal helices against the five-stranded β-sheet was evidenced by NOE connectivities between residues in α_1 and residues in β_1 and β_2 and between residues in α_3 and residues in β_5, β_6, and β_7. On the other side of the sheet residues in α_2 displayed close

Figure 3. (*A*) Ribbon diagram of profilin-I showing the side chains of Lys[115] (*green*) and of the 17 residues conserved in at least five of the following six phyla; protista (*Acanthamoeba*), myxomycete (*Physarum*), fungi (yeast), echinoderm, vertebrate and vaccinia virus (*red*). (*B*) Ribbon diagram of profilin-I showing the side chains of the 22 residues that differ between *Acanthamoeba* profilins-I and II (*yellow* or *purple*). Residues which involve a potential charge difference between profilins-I and II are colored purple.

contacts to residues in β_5, β_6, and β_7, whereas residues in the two-stranded β-sheet were close to residues in β_5 and β_6.

Discussion

The NMR structural studies of profilin indicate that the protein has a well-defined, compact structure in solution. The three-dimensional structure of profilin also provides information relating the structure of this protein with its biological activities.

The location of the actin binding site is clearly delineated by the tertiary structure of the protein. Three lines of evidence indicate that the face of profilin consisting of the NH_2- and COOH-terminal helices participates in binding actin monomers. First, Lys^{115} (Fig. 3 *A*) in the carboxy terminal helix of *Acanthamoeba* profilin-I or II can be cross-linked to Glu^{364} of actin through a zero length isopeptide bond (Vanderkerckhove et al., 1989). Second, the actin binding proteins fragmin, gelsolin and severin contain sequences that are homologous to ~30 residues at the carboxy terminus of *Acanthamoeba* profilin (Ampe and Vanderkerckhove, 1987; Andre et al., 1988). Third, although profilin sequences vary considerably across the phylogenetic tree, 14 of the 17 most widely conserved residues (Pollard and Rimm, 1991; Tagaki et al., 1990) are located on or adjacent to the NH_2- and COOH-terminal helices. 16 of these residues are conserved in *Acanthamoeba* profilin-I (Fig. 3 *A*). The conserved residues include the aromatic side chains Trp^2, Trp^{29}, and Tyr^5; the hydrophobic residues Leu^{10}, Leu^{120}, and Ile^{21}; the charged residue Asp^7 and four glycine residues Gly^{12}, Gly^{59}, Gly^{64}, and Gly^{107}. The conformations of the Trp residues are particularly interesting as these could be used as fluorescent probes to study interactions between profilin and other molecules. In the NMR structures of *Acanthamoeba* profilin-I the aromatic side chain of Trp^2 is buried while the side chain of Trp^{29} is close to the surface of the protein. Trp^2 is in close proximity to the conserved residues Leu^{120}, Ala^{117}, Tyr^5, and Thr^{91}. In *Acanthamoeba* profilin-I, two of the conserved residues, Gly^{59} and Gly^{64}, are located on the opposite side of the β-sheet from the other 14 conserved residues; these glycines may be important for maintaining structural elements of profilins.

The tertiary structure of profilin-I also provides information about the binding of profilin-I and II to phosphoinositides. Although profilins have similar affinities for actin, the binding constants for PIP_2 vary among profilins. For example, both *Acanthamoeba* profilin-II and human platelet profilin have a higher affinity (K_d = 3 μM) for PIP_2 than profilin-I (K_d = 100 to 500 μM) (Machesky et al., 1990). The 22 amino acid differences between *Acanthamoeba* profilins-I and II (Pollard and Rimm, 1991) are colored yellow or purple in Fig. 3 *B*. Most of the variable residues are localized on the side of the molecule opposite the postulated actin binding region. Nine of the amino acid changes are conservative substitutions; these involve four hydrophobic residues, four polar residues and one charged residue. Of the nonconservative substitutions the most interesting are those resulting in a charge difference since binding of profilin to negatively charged lipids is likely to involve electrostatic interactions. The residues colored purple in Fig. 3 *B* differ in charge between profilin-I and II, namely 24 (Leu/His), 50 (Asn/Lys), 51 (Asn/Asp) and 53 (Asp/Thr). These amino acid substitutions give profilin-II a net positive charge 1–2 units greater than profilin-I. The exact difference cannot be calculated as the charge on His^{24} in profilin-II is unknown. The amino acid change at residue 66 (His/Arg) could also potentially result in a charge difference. However, we have determined by NMR that the charge on His^{66} of profilin-I is +1 at pH 7.4, which is above the cytoplasmic pH in *Acanthamoeba*. The two neutral residues in profilin-I (Leu^{24} and Asn^{50}), which are replaced by positively charged residues in profilin-II, are solvent exposed and are close to the basic residues Lys^{90} and Lys^{93}. Leu^{24} is in the loop between β strands 1 and 2, Asn^{50} is the residue immediately succeeding helix 2, Lys^{90} is at the COOH-terminal end of β-strand 6 and Lys^{93} is in the loop between β-strands 6 and 7. Together these residues form a basic cluster at the base of the molecule (where the orientation is as shown in the figures), on the side adjacent to the NH_2- and COOH-terminal helices. This provides a potential lipid binding site in profilin-II. In the profilin sequence alignment presented by Pollard and Rimm (1991) the four variably charged residues in *Acanthamoeba* profilin have the same charge in profilin-II and vertebrate profilin, which have similar affinities for PIP_2. Considering the wide variance in primary sequence between these two profilins it will be interesting to learn whether the spatial positions of these residues are conserved once a tertiary structure of vertebrate profilin is available.

Although the proposed binding sites for actin and PIP_2 are not on the same face of the profilin molecule, PIP_2 inhibits the binding of actin (Lassing and Lindberg, 1985, 1988; Goldschmidt-Clermont et al., 1991*b*). Assuming that we have identified the binding sites correctly, we think that the simplest explanation is that the two large ligands actually interfere sterically with each other. In the orientation shown in Fig. 3 *B*, the basic residues of profilin-II that are suggested to bind PIP_2 are on the bottom of the model, while the COOH-terminal actin-binding helix is on the adjacent face. If a large bound actin molecule overhangs the edges of the small profilin molecule, then actin may not have full access to its binding site when profilin is associated with a planar lipid bilayer or even a PIP_2 micelle. Alternatively, binding of either or both actin and PIP_2 may involve conformational changes (Raghunathan et al., 1992) that preclude binding of the other ligand. Further structural studies of profilin-actin and profilin-lipid complexes will be required to address these questions.

Further NMR experiments promise to be a particularly valuable adjunct to the high resolution x-ray crystal structure of profilin being pursued by us and other investigators because this NMR structure can be used for phasing by molecular replacement. Moreover, NMR experiments evaluating hydrogen exchange protection and chemical shift perturbations in the presence of phospholipids, polyproline, and actin should identify profilin residues involved in interactions with these molecules. Such results will help to elucidate the relationship between profilin structure and function.

We gratefully acknowledge G. Vuister for acquisition and processing of the four-dimensional NOESY spectrum; D. Garrett, S. Grzesiek, and F. Delaglio for providing computer software; R. Tschudin for technical support; R. Powers and T. Yamazaki for help with XPLOR; J. Cammisa and B. K. Lee for photography; and A. Bax for helpful discussions.

This work was supported by National Institutes of Health Research Grant GM-35171 (to E. E. Lattman and T. D. Pollard), the AIDS Targeted

Antiviral Program of the Office of the Director of the National Institutes of Health (to D. A. Torchia), and Public Health Service National Research Service Award GM13620 (to S. J. Archer).

Received for publication 1 June 1993 and in revised form 24 June 1993.

Note added in proof: Since submission of this manuscript, better refined structures have been generated using additional NOEs and stereospecific assignments of sidechains. In these structures the region succeeding the first helix is well constrained and has helical character. In addition the COOH-terminal helix is longer, starting at residue Pro106.

References

Ampe, C., and J. Vandekerckhove. 1987. The F-actin capping proteins of Physarum polycephalum:cap42(a) is very similar, if not identical, to fragmin and is structurally very homologous to gelsolin; cap42(b) is physarum actin. *EMBO (Eur. Mol. Biol. Organ.) J.* 6:4149–4157.

Ampe, C., J. Vandekerckhove, S. Brenner, L. Tobacman, and E. Korn. 1985. The amino acid sequence of *Acanthamoeba* profilin. *J. Biol. Chem.* 260: 834–840.

Andre, E., F. Lottspeich, M. Schleicher, and A. Noegel. 1988. Severin, gelsolin, and villin share a homologous sequence in regions presumed to contain F-actin severing domains. *J. Biol. Chem.* 236:722–727.

Archer, S. J., M. Ikura, D. A. Torchia, and A. Bax. 1991. An alternative 3D NMR technique for correlating backbone ^{15}N with side chain Hβ resonances in larger proteins. *J. Magn. Reson.* 95:636–641.

Archer, S. J., V. K. Vinson, T. D. Pollard, and D. A. Torchia. 1993. Secondary structure and topology of *Acanthamoeba* profilin I as determined by heteronuclear NMR spectroscopy. *Biochemistry*. In press.

Brünger, A. T. 1992. X-PLOR Manual Version 3.0: A System for Crystallography and NMR. Yale University Press, New Haven, CT. 405 pp.

Carlsson L., L. Nystrom, I.Sundkvist, F. Markey, and U. Lindberg. 1977. Actin polymerizability is influenced by profilin, a low molecular weight protein in non-muscle cells. *J. Mol. Biol.* 115:465–483.

Clore, G. M., A. Bax, P. T. Wingfield, and A. M. Gronenborn. 1990. Identification and localization of bound internal water in the solution structure of interleukin 1β by heteronuclear three-dimensional ^{1}H rotating frame Overhauser effect ^{15}N-^{1}H multiple quantum coherence NMR spectroscopy. *Biochemistry*. 29:5671–5676.

Clore, G. M., and A. M. Gronenborn. 1989. Determination of three-dimensional structures of proteins and nucleic acids in solution by nuclear magnetic resonance spectroscopy. *Crit. Rev. Biochem. Mol. Biol.* 24:479–564.

Clore, G. M., and A. M. Gronenborn. 1991. Structures of larger proteins in solution: three- and four-dimensional heteronuclear NMR spectroscopy. *Science (Wash. DC).* 252:1390–1399.

Clore, G. M., A. M. Gronenborn, M. Nilges, and C. A. Ryan. 1987. Three-dimensional structure of potato carboxypeptidase inhibitor in solution. A study using nuclear magnetic resonance, distance geometry, and restrained molecular dynamics. *Biochemistry*.26:8012–8013.

Clore, G. M., M. Nilges, D. K. Sukumaran, A. T. Brünger, M. Karplus, and A. M. Gronenborn. 1986. The three-dimensional structure of α1-purothionin in solution: combined use of nuclear magnetic resonance, distance geometry and restrained molecular dynamics. *EMBO (Eur. Mol. Biol. Organ.) J.* 5:2729–2735.

Goldschmidt-Clermont, P., J. Kim, L. Machesky, S. Rhee, and T. Pollard. 1991*a*. Regulation of Phospholipase C-γ1 by profilin and tyrosine phosphorylation. *Science (Wash. DC).* 251:1231–1233.

Goldschmidt-Clermont, P., L. Machesky, S. Doberstein, and T. Pollard. 1991*b*. Mechanism of the interaction of human platelet profilin with actin. *J. Cell Biol.* 113:1081–1089.

Goldschmidt-Clermont, P. J., L. M. Machesky, J. J. Baldassare, and T. D. Pollard. 1990. The actin-binding protein profilin binds to PIP_2 and inhibits its hydrolysis by phospholipase C. *Science (Wash. DC).* 247:1575–1578.

Haarer, B., S. Lillie, A. Adams, V. Magdolen, W. Bandlow, and S. Brown. 1990. Purification of profilin from *Saccharomyces cerevisiae* and analysis of profilin-deficient cells. *J. Cell Biol.* 110:105–114.

Kaiser, D. A., M. Sato, R. F. Ebert, and T. D. Pollard 1986. Purification and characterization of two isoforms of *Acanthamoeba* profilin. *J. Cell. Biol.* 102:221–226.

Kay, L. E., and A. Bax. 1990. New NMR methods for the measurement of NH-CαH coupling constants in ^{15}N-labeled proteins. *J. Magn. Reson.* 86:110–126.

Kraulis, P. 1991. MOLSCRIPT, a program to produce both detailed and schematic plots of protein structures. *J. Appl. Crystallogr.* 24:946–950.

Lassing, I., and U. Lindberg. 1985. Specific interaction between phosphatidylinositol 4,5-biphosphate and profilactin. *Nature (Lond.).* 314:472–474.

Lassing, I., and U. Lindberg. 1988. Specificity of the interaction between PIP_2 and the profilin:actin complex. *J. Cell. Biochem.* 37:255–267.

Machesky, L. M., P. J. Goldschmidt-Clermont, and T. D. Pollard. 1990. The affinities of human platelet and *Acanthamoeba* profilin isoforms for polyphosphoinositides account for their relative abilities to inhibit phospholipase C. *Cell Regul.* 1:937–950.

Magnus, K. A., E. E. Lattman, M. Sato. and T. D. Pollard. 1986. Crystallization of *Acanthamoeba* profilin-I. *J. Biol. Chem.* 261:13360–13361.

Marion, D., L. E. Kay, S. W. Sparks, D. A. Torchia, and A. Bax. 1989. Three-dimensional heteronuclear NMR of ^{15}N-labeled proteins. *J. Am. Chem. Soc.* 111:1515–1517.

Mockrin, S., and E. Korn. 1980. *Acanthamoeba* profilin interacts with G-actin to increase the exchange of actin bound adenosine 5′ triphosphate. *Biochemistry*. 19:5359–5362.

Nilges, M., G. M. Clore, and A. M. Gronenborn. 1988. Determination of three-dimensional structures of proteins from interproton distance data by dynamical simulated annealing from a random array of atoms. *FEBS (Fed. Eur. Biochem. Soc.) Lett.* 229:317–324.

Nishida, E. 1985. Opposite effects of cofilin and profilin from porcine brain on rate of exchange of actin-bound adenosine 5′-triphosphate. *Biochemistry.* 24:1160–1164.

Pollard, T., and J. Cooper. 1986. Actin and actin-binding proteins. A critical evaluation of mechanisms and functions. *Annu. Rev. Biochem.* 55:987–1035.

Pollard, T. D., and J. A. Cooper. 1984. Quantitative analysis of the effect of *Acanthamoeba* profilin on actin filament nucleation and elongation. *Biochemistry*. 23:6631–6641.

Pollard, T. D., and D. L. Rimm. 1991. Analysis of cDNA clones for *Acanthamoeba* profilin-I and profilin-II shows end to end homology with vertebrate profilins and a family of profilin genes. *Cell Motil. Cytoskel.* 20:169–177.

Raghunathan, V., P. Mowery, M. Rozycki, U. Lindberg, and C. Schutt. 1992. Structural changes in profilin accompany its binding to phosphatidylinositol 4,5-biphosphate. *FEBS (Fed. Eur. Biochem. Soc.) Lett.* 297:46–50.

Reichstein, E., and E. D. Korn. 1979. *Acanthamoeba* profilin (a protein of low molecular weight from *Acanthamoeba* that inhibits actin nucleation). *J. Biol. Chem.* 254:6174–6179.

Schutt, C. E., U. Lindberg, J. Myslik, and N. Strauss. 1989. Molecular packing in profilin: actin crystals and its implications. *J. Mol. Biol.* 209:735–746.

Tagaki, T., I. Mabuchi, H. Hosoya, K. Furuhashi, and S. Hatano. 1990. Primary structure of profilins from two species of Echinoidea and Physarum polycephalum. *Eur. J. Biochem.* 192:777–781.

Tanaka, M., and H. Shibata. 1985. Poly (L-proline)-binding proteins from chick embryos are profilin and profilactin. *Eur. J. Biochem.* 151:291–297.

Vanderkerckhove, J. S., D. A. Kaiser, and T. D. Pollard. 1989. *Acanthamoeba* actin and profilin can be cross-linked between glutamic acid 364 of actin and lysine 115 of profilin. *J. Cell Biol.* 109:619–626.

Vojtek, A., B. Haarer, J. Field, J. Gerst, T. D. Pollard, S. Brown, and M. Wigler. 1991. Evidence for a functional link between profilin and CAP in the yeast *S. cerevisiae*. *Cell.* 66:497–505.

Vuister, G., and A. Bax. 1993. Quantitative J correlation: a new approach for measuring homonuclear three-bond $J(H^{N}H^{\alpha})$ coupling constants in ^{15}N-enriched proteins. *J. Am. Chem. Soc.* In press.

Wüthrich, K. 1989. Protein structure determination in solution by nuclear magnetic resonance spectroscopy. *Science (Wash. DC).* 243:45–50.

Wüthrich, K., M. Billetter, and W. Braun. 1983. Pseudo-structures for the 20 common amino acids for use in studies of protein conformations by measurements of intramolecular proton-proton distance constraints with nuclear magnetic resonance. *J. Mol. Biol.* 169:949–961.